The Korean Journal of Rheology,
Vol. 10, No. 2, June 1998 pp. 65-73

<연구논문>

삼중블록공중합체와 저분자량 단일중합체 혼합물의 미세상분리 동력학

이승헌 · 차국헌
서울대학교 화학공학과
(1998년 4월 8일)

Ordering Kinetics of Triblock Copolymer/Low Molecular Weight Homopolymer Mixtures

Seung Heon Lee and Kookheon Char
Department of Chemical Engineering, Seoul National University, Seoul 151-742, Korea
(Received April 8, 1998)

요 약

본 연구에서는 polystyrene-*block*-poly(ethylene-*co*-butylene)-*block*-polystyrene (SEBS) 삼중블록공중합체와 저분자량 단일중합체인 Hercotac 1149 (H1149)의 70/30 (w/w) 혼합물의 미세상분리와 그 동력학을 유변물성 측정법과 SAXS 실험을 통하여 연구해 보았다. 먼저 혼합물의 미세상분리 온도를 유변물성 측정법과 SAXS 실험을 통해 각각 구한 다음, 샘플을 미세상분리 온도보다 높은 온도에서 그 이하의 온도로 급냉시킨 후 유변물성과 산란강도의 시간에 따른 변화로부터 미세상분리 동력학에 대한 정보를 구하였다. 이렇게 얻어진 데이터를 Avrami 형태의 핵생성 성장 (NG) 메커니즘으로 해석해 보았는데, 최대산란강도 I_{max} 뿐만 아니라 저장 점탄성계수 G'과 손실 점탄성계수 G"의 시간에 따른 변화를 잘 예측할 수 있었다. 한편, 서로 다른 두 time-resolved 실험으로부터 Avrami 플롯을 그려서 구해진 Avrami 변수들은 같은 급냉 깊이에서는 서로 잘 일치함을 확인하였다. 반감기는 급냉 깊이가 증가함에 따라 점차 감소하는 경향을 보였는데, 이는 급냉 깊이가 클수록 미세상분리가 더 빨리 진행되고 있음을 보여주는 것이다. 또한, Avrami 지수는 급냉 깊이가 증가함에 따라 3에서 4로 급격히 변했는데, 이로부터 급냉 깊이가 작을 때에는 70/30 (w/w) SEBS/H1149 혼합물의 미세상분리가 불균일 핵생성 성장 메커니즘에 따라 진행되고, 급냉 깊이가 더 커지면 미세상분리가 스피노달 상분리 메커니즘으로 변하고 있음을 예측할 수 있었다.

Abstract—The order-disorder transition (ODT) and the ordering kinetics of a 70/30 (w/w) mixture of polystyrene-*block*-poly (ethylene-*co*-butylene)-*block*-polystyrene (SEBS), Kraton G1652, and a commercial tackifier, Hercotac 1149 (H1149) was investigated using both *time-resolved* rheological and *synchrotron* small-angle X-ray scattering (SAXS) measurements. T_{ODT} of the mixture was first determined independently by each static measurement. Time-resolved measurements were then carried out by quenching the sample from disordered to ordered state. The time-resolved data were analyzed based on the nucleation and growth (NG) mechanism of the Avrami class. It was found that the NG mechanism reasonably describes the time evolution of G' and G" as well as I_{max} for the 70/30 (w/w) mixture after a given quench except the initial induction period. The Avrami parameters obtained from both time-resolved measurements based on the NG mechanism (Avrami plots) were found to be in good agreement with each other for the same quench depth. The half-time was found to decrease gradually as the quench depth was increased, indicating that the ordering proceeds faster for a deeper quench. The Avrami exponent was found to change suddenly from about 3 to 4 in going from a shallow to a deeper quench. This implies that for a shallow quench the ordering of 70/30 (w/w) mixture proceeds *via* the heterogeneous NG mechanism, while there exists a transition in the ordering kinetics into the spinodal decomposition (SD) mechanism when the sample is further quenched.
Keywords: block copolymer/homopolymer mixture, order-disorder transition (ODT), ordering kinetics, time-resolved rheological measurement, time-resolved small-angle X-ray scattering (SAXS)

1. Introduction

Block copolymers have attracted many researchers since they can self-organize into various microphase separated structure in the order of a few hundred Å below a certain critical temperature that is called the *microphase separation* temperature (T_{MST}) or *order-disorder transition* temperature (T_{ODT}). One of the main issues in the design of block copolymers is to control their microdomain morphology since they in turn strongly affect final physical properties. The preparation of well-defined block copolymers has been accomplished *via* careful synthesis

such as anionic polymerization, but synthesizing a block copolymer with a precise block composition is, even though possible, quite tedious. This laborious task can be avoided simply by adding a small amount of homopolymer to the block copolymer. If the molecular weight of homopolymer is sufficiently low and the homopolymer is selectively more miscible with one of the blocks than the other, the homopolymer tends, to a large extent, to be solubilized into one of the microdomains[1-3]. In this case, the macrophase separation between constituent polymers is suppressed and the microphase separation becomes dominant. Consequently, one can focus only on the order-disorder transition (ODT) and/or the ordering kinetics.

There have been many theoretical and experimental investigations on the ODT of pure block copolymers[4-10]. Ordering kinetics of block copolymers have also been investigated by some researchers. Earlier works were done by Hashimoto and coworkers[11,12]. Assuming that the microphase dissolution at T_{ODT} was attained by the Brownian motion of centers of block copolymer, they explored the dynamics of polystyrene-polybutadiene (SB) diblock copolymers in C14 with various compositions after a temperature jump from the ordered to the disordered state using time-resolved SAXS measurements. Hashimoto[13] further extended his work to the ordering kinetics of block copolymers based on the time-dependent Ginzburg-Landau approach and proposed that the ordering of block copolymers could proceed *via* spinodal decomposition. More recent works reported that the ordering process occurs *via* nucleation and growth (NG) mechanism when the block copolymer is quenched just below T_{ODT} where the composition fluctuation effects play an important role. Fredrickson and Binder[14] developed a theory which describes the nucleation and growth of weakly inhomogeneous lamellar phase from a supercooled disordered phase. Assuming composition fluctuation near the order-disorder transition and neglecting time lag effect, they were able to derive a classical Avrami type equation with an exponent n = 4 for the ordering of a symmetric diblock copolymer (f=1/2, f is the volume fraction of one block in the block copolymer). The homogeneous nucleation barrier for a symmetric diblock copolymer was predicted to be unusually small,

$$\Delta F^*/k_BT \sim \bar{N}^{-1/3}\delta^{-2} \quad (1)$$

where $\bar{N}$ is the Ginzburg parameter which is proportional to the degree of polymerization of block copolymer and δ is the degree of undercooling defined as $\delta \equiv (\chi-\chi_{ODT})/\chi_{ODT} \sim (T_{ODT}-T)/T$. The equivalent expression for an asymmetric diblock copolymer ($f \neq 1/2$) was predicted to be quite different[15],

$$\Delta F^*/k_BT \sim \bar{N}^{1/2}|f-0.5|^5\delta^{-2} \quad (2)$$

Experimentally, Rosedale and Bates[6] measured the time evolution of G' for a poly(ethylene-*alt*-propylene)-polyethylethylene (PEP-PEE) diblock copolymer (f_{PEP}=0.55) after quenching the sample just below T_{ODT}, and showed that their time-dependent rheological results could be analyzed by the heterogeneous nucleation and growth kinetics. Hashimoto and Sakamoto[16] used time-resolved SAXS and TEM to investigate the ordering kinetics of a symmetric polystyrene-polyisoprene (SI) diblock copolymer. Their results again supported that for a shallow quench the ordering of the lamellar microdomains proceeded *via* the nucleation and growth mechanism. Similar results were reported by Floudas and coworkers using time resolved rheology and/or SAXS for a symmetric SI diblock copolymer[17], SI_2 3-mikoarm star copolymers and SIB terpolymers[18], and $(SI)_n$ star copolymers[19]. They also examined the ordering kinetics of miscible binary blends of lamellar SI diblock copolymers with different molecular weights[20]. Changing blend composition, thus varying the effective degree of polymerization, they found that the characteristic time for the ordering scales as $\bar{N}^{1/3}$, in agreement with Fredrickson and Binder's predictions[14]. Adams *et al.*[21] reported that the ordering dynamics of asymmetric (13 wt% styrene) SI diblock and SIS triblock copolymers were significantly slower than those of nearly symmetric SI diblock copolymers with similar T_{ODT}, as evidenced from time-resolved SAXS and rheological data. Other research groups also investigated the ordering kinetics of different systems[22-24].

While much literature is available on the ODT of block copolymers and some on the ordering kinetics of block copolymers, there have been few studies on the ordering kinetics of block copolymer/homopolymer mixtures. Since block copolymer/homopolymer mixtures are presently gaining more attention in industrial applications such as pressure sensitive adhesives, it is necessary to understand their ODT behavior and the ordering kinetics.

In present study, we investigated the ordering kinetics of a block copolymer/low molecular weight homopolymer (SEBS/H1149) mixture with a specific composition using both *time-resolved* rheological and *synchrotron* small-angle X-ray scattering (SAXS) measurements. T_{ODT} of the

mixture was first determined independently by each static measurement. Time-resolved measurements were then carried out by quenching the sample from disordered to ordered state. The time-resolved data were analyzed based on the nucleation and growth (NG) mechanism of the Avrami class. Results obtained from two independent time-resolved experiments were compared with each other.

2. Experimental

2.1. Materials

A commercial grade of polystyrene-*block*-poly(ethylene-*co*-butylene)-*block*-polystyrene (SEBS) copolymer, Kraton G1652 (Shell Development Co.), and a commercially available tackifying resin (H1149), Hercotac 1149 (Hercules Co.), were used as received. The characteristics of polymers used in present study are summarized in Table 1. Kraton G1652/Hercotac 1149 mixture will be hereafter denoted as SEBS/H1149 mixture.

2.2. Sample Preparation

70/30 (w/w) SEBS/H1149 mixture was prepared by solution casting method with toluene as a solvent. Predetermined amounts of SEBS block copolymer and H1149 homopolymer were first dissolved in toluene (15 wt% solid content) together with 0.2 wt% of antioxidant (Irganox 1076, Ciba-Geigy Group), and then the solvent was slowly evaporated. The evaporation of the solvent was first carried out in open air at room temperature for 3 weeks and then in a vacuum oven at 60°C for 3 days. Finally, the samples were annealed in a vacuum oven at 130°C for 3 days. The thickness of the samples obtained was about 2 mm. No evidence for macrophase separation was found for the mixture over the entire temperature range covered in this experiment, which was confirmed by a hot-stage microscopy.

The samples for synchrotron small-angle X-ray scattering (SAXS) measurements were prepared by filling as-cast specimens into sample holders made of brass (0.8 mm inner diameter with 2 mm thickness) and then sealing both sides by thin imide films.

Table 1. Characteristics of polymers used in this study

Sample code	Structure	$\overline{M}_w \times 10^{-3}$	$\overline{M}_w/\overline{M}_n$	wt% of PS block
Kraton 1652[a]	SEBS[b] triblock copolymer	7.0-b-37.5-b-7.0	1.09	27.2
Hercotac 1149[c]	Aromatically modified C5 resin	2.02	1.93	–

[a]Supplied by Shell Chemical Co.
[b]Polystyrene-*block*-poly(ethylene-*co*-butylene)-*block*-polystyrene
[c]Supplied by Hercules, Inc.

2.3. Rheology

RMS 800 (Rheometrics Inc.) in parallel plate geometry (25 mm diameter and 1.5 mm gap) was used to measure the dynamic viscoelastic storage and loss moduli, G' and G", of the mixture as functions of angular frequency, ω, and temperature, T. In order to determine the order-disorder transition temperature (T_{ODT}) of the mixture, isochronal temperature scans at a fixed frequency were carried out at a heating rate of 2°C/min. Strain amplitude was small enough to ensure linear viscoelasticity (typically below 5%). All measurements were carried out under nitrogen blanket in order to prevent oxidative degradation of the samples.

Isochronal/isothermal time scans were also carried out for the 70/30 (w/w) SEBS/H1149 mixture. First, temperature was raised about 15°C above T_{ODT} of the sample, which was determined from the isochronal measurement, and maintained for 10 min to ensure thermal equilibrium. The sample was then rapidly quenched below T_{ODT}, thus enabling the ordering to proceed. Time evolutions of G' and G" were monitored immediately after quenching.

2.4. Synchrotron Small-Angle X-ray Scattering (SAXS)

Synchrotron SAXS measurements were carried out at X-ray scattering beamline in Pohang Light Source (PLS), which consisted of a 2 GeV LINAC accelerator, a storage ring, Si(111) double crystal monochromators, ion chambers and a one-dimensional linear position sensitive detector (EG&G 1612XR w/ OMA) with 1024 pixels. The wavelength (λ) of synchrotron beam was 1.59 Å and the energy resolution ($\Delta\lambda/\lambda$) was 5×10^{-4}. Typical beam size was smaller than 1×1 mm^2. Sample-to-detector distance was 90.1 cm. Data were obtained by SPEC data acquisition S/W operating on a PC. SAXS profiles obtained were corrected for absorption, air scattering and imide film scattering.

Two types of SAXS measurements were conducted for the 70/30 (w/w) SEBS/H1149 mixture: (1) static SAXS measurements at different temperatures to determine T_{ODT} of the mixture and (2) time-resolved SAXS measurements to study the ordering kinetics of the mixture. In static measurements, temperature was raised stepwise to ensure that the sample achieves thermal equilibrium. The temperature of the 70/30 (w/w) mixture was initially set to

242°C and maintained for 10 min, and then the sample was slowly heated to the next temperature (245°C) at a ramping rate of 1°C/min, and then it was maintained at the set temperature for 3 min and so on. Each SAXS measurement was conducted 1 min before the next ramping. Data acquisition time for each static measurement was 30 sec, which is sufficient to minimize statistical errors in data acquisition.

In time-resolved SAXS measurements for the 70/30 (w/w) mixture, the sample temperature was initially set using a heating stage about 10°C above T_{ODT} of the sample, which was determined from the static measurements, and maintained for 30 min to ensure thermal equilibrium. The sample was then rapidly quenched by moving it into another heating stage maintained at a temperature below T_{ODT}, thus enabling us to monitor the ordering as a function of time. Immediately after the quenching, the scattering intensity profiles of the sample were measured every 20 sec. Data acquisition time for each dynamic measurement was 5 sec.

3. Results and Discussion

3.1. ODT Determination of 70/30 (w/w) SEBS/H1149 Mixture

Before jumping directly into the ordering kinetics of our triblock copolymer/homopolymer mixture, it is first necessary to determine the ODT temperature (T_{ODT}). We employed here two different methods, rheological and scattering measurements, to determine the T_{ODT} of the mixture.

Fig. 1 shows the change in dynamic storage modulus, G', of a 70/30 (w/w) SEBS/H1149 mixture with temperature during a heating cycle. Heating rate was 2°C/min, angular frequency was 0.5 rad/s and the stain applied was well within linear viscoelastic region (~2.5%). In Fig. 1, it can be clearly seen that there is an abrupt drop in G' around 246°C. Rosedale and Bates[6] investigated the order-disorder transition behavior of a series of PEP-PEE block copolymers with lamellar microdomains and they found that both G' and G" drop precipitously at a certain temperature with angular frequencies below critical values (ω_c' and ω_c'' respectively). They also reported that the drop in G' is more pronounced since the critical angular frequency for G' is larger than that for G" (i.e., $\omega_c'>\omega_c''$). According to their criterion, the temperature at which there was an abrupt drop in G' was chosen as T_{ODT} of the 70/30 (w/w) SEBS/H1149 mixture. It should be mentioned here that the drop in G' is not so sharp. There are two possible reasons for this: First, the angular frequency employed in our study may not be small enough to ensure $\omega<\omega_c'$. Second, the heating rate used here (2°C/min) may be large.

Fig. 2 shows a series of SAXS intensity profiles for 70/30 (w/w) SEBS/H1149 mixture with a stepwise temperature increment of ca. 3°C. At low temperatures the mixture demonstrates a sharp first-order scattering peak resulting from the periodicity of microdomains of the mixture, while at high temperatures it shows a broad peak which is due to the "correlation hole" effect in the disordered state. The SAXS intensity profile of the 70/30 (w/w) mixture decreased gradually as temperature was raised but at a certain

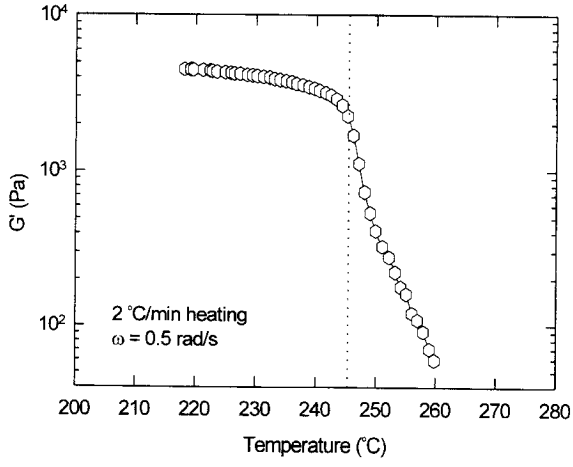

Fig. 1. Temperature dependence of G' measured at ω=0.5 rad/s when 70/30 (w/w) SEBS/ H1149 mixture was heated at 2°C/min. Strain was fixed at 2.5%.

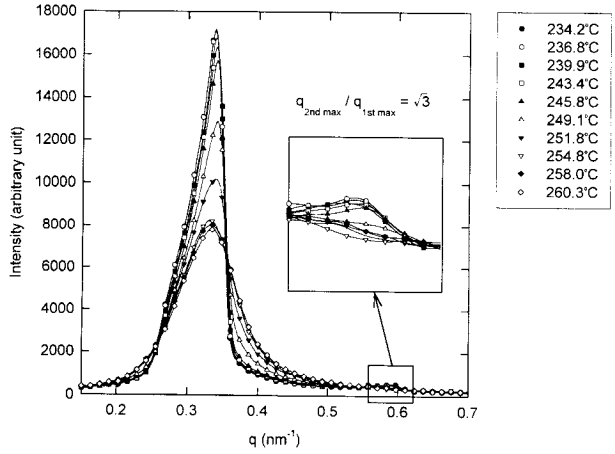

Fig. 2. Synchrotron SAXS profiles for 70/30 (w/w) SEBS/H1149 mixture at different temperatures. The rectangular area where the second-order scattering peaks appear is enlarged in the inset.

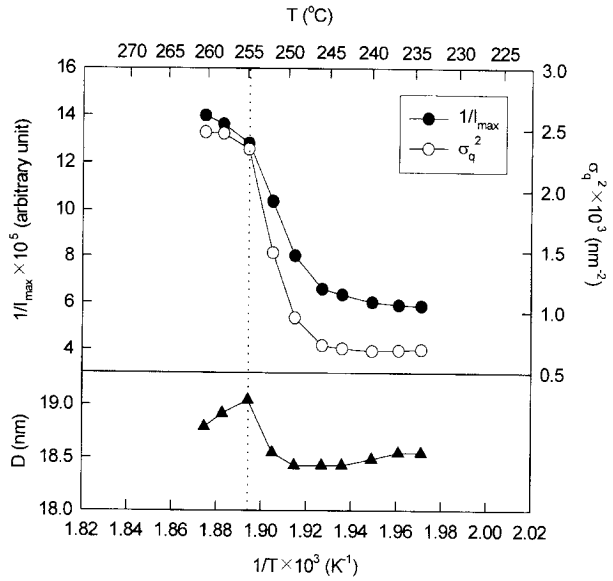

Fig. 3. Temperature dependences of scattering parameters for 70/30 (w/w) SEBS/H1149 mixture: (a) $1/I_{max}$ and σ_q^2 versus 1/T and (b) D versus 1/T.

critical temperature the sharp maximum was rapidly converted into a broad maximum. The discontinuity can be seen more clearly when the inverse of the first-order scattering maximum, $1/I_{max}$, and the square of the half-width at half-maximum (HWHM), σ_q^2, are plotted against inverse temperature, 1/T, as shown in Fig. 3a. There is an abrupt drop in $1/I_{max}$ as well as in σ_q^2 over a temperature range between 245.8°C and 254.8°C, but the drop in σ_q^2 is more pronounced than that in $1/I_{max}$. The values of σ_q^2 are more reliable experimentally than those of $1/I_{max}$ because they are free from errors during absolute intensity corrections of the SAXS data. Recently, Sakamoto and Hashimoto[8] also found that the SAXS profiles for SI diblock copolymers changed dramatically at $T=T_{ODT}$, showing a sharp decrease in the first-order scattering peak. Based on their SAXS results, they proposed a "unified view" on ODT; $1/I_{max}$ as well as σ_q^2 shows a discontinuity at ODT when plotted against 1/T. According to their criterion, the temperature range showing a discontinuous change was chosen as the T_{ODT} of the 70/30 (w/w) mixture determined by the SAXS measurement. It should, however, be mentioned here that the drop is rather broad compared with the sharp discontinuity at ODT reported by other investigators[8,18,19]. This may be due to the poor temperature resolution of current SAXS measurements. Ogawa *et al.*[26] reported that a tiny temperature increment (e.g. 1°C) is required in order to observe a sharp discontinuity in $1/I_{max}$ as well as in σ_q^2. It seems that the temperature increment, 3°C, chosen in this measurement was not sufficient to locate the exact value of T_{ODT}. Another possibility is that the broad molecular weight distribution (or large polydispersity index, ca. 1.93) of low molecular weight homopolymer, Hercotac 1149, gives rise to a rather broad discontinuity in SAXS parameters. Fig. 3b shows the change of the microdomain periodicity in ordered state or the dominant fluctuation mode in disordered state (D) defined as $2\pi/q_{max}$ for the 70/30 (w/w) mixture as a function of temperature. A clear discontinuity at ODT is also observed.

In addition to the discontinuities of the scattering parameters at ODT, there is one more evidence for the ODT. In Fig. 2, you may be able to see an additional scattering peak at ca. $q=0.59$ nm^{-1} although its intensity is much weaker than that of the first-order scattering peak. In order to see the intensity change of the peak more clearly, the portion was enlarged in the inset of Fig. 2. It is interesting to note that the additional second-order scattering peak disappears above 245.8°C which is the onset temperature of ODT for the 70/30 (w/w) SEBS/H1149 mixture determined by observing abrupt drops in $1/I_{max}$ and σ_q^2 with increasing 1/T. Multiple-order scattering maxima are the characteristics of microphase separated domains having long-range orders. This is, however, beyond the scope of this paper, and will not be discussed any further.

As evident from Fig. 's 1 and 3, there is a slight difference between the values of the ODT temperatures determined by rheology and SAXS. This is mainly due to the difference in temperature resolution of the two measurements.

3.2. Time-resolved Rheoloy and SAXS

Isochronal/isothermal time scans were employed in time-resolved rheology. Fig. 4 shows the time evolutions of G' and G" measured at 0.5 rad/s for the 70/30 (w/w) mixture after quenching the sample from 260°C (about 15°C above T_{ODT}) to a given temperature. Strain was fixed at 3%. Both G' and G" show sigmoidal shapes with two plateaus at short and long times: both G' and G" initially grow rapidly to the first plateau immediately after quenching, and then increase gradually to the second plateau. The initial induction period originates from the fact that the sample temperature does not drop stepwise but rather change gradually over a short time period, as will be discussed below in more detail. The plateau values of G' and G" at short times are assumed to represent the rheological properties of the disordered phase at the final temperature[17]. On the other hand, the plateau values at long times signify

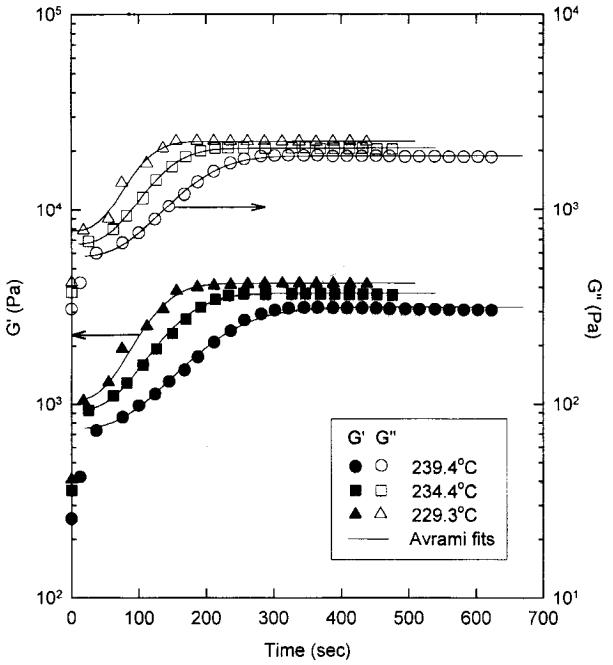

Fig. 4. Time evolutions of G' and G" for 70/30 (w/w) SEBS/H1149 mixture after quenching the sample from 260°C to a given temperature. Solid lines are the best fits to the Avrami equations (Eqs. 4 and 6).

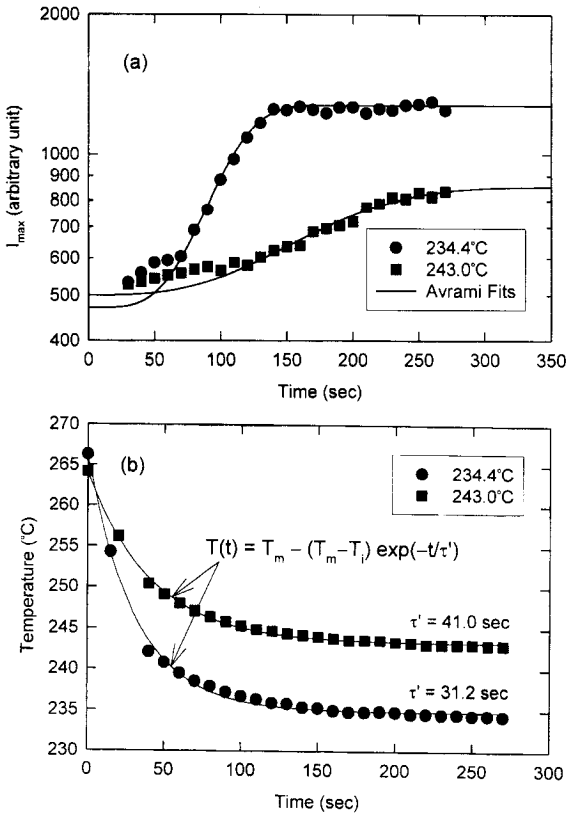

Fig. 5. (a) Time evolution of I_{max} for 70/30 (w/w) SEBS/H1149 mixture for two quench depths. Solid lines are the best fits to the Avrami equations (Eqs. 5 and 6). (b) Change of temperature of the SAXS sample as a function of time after quenching into two different final temperatures. The solid lines are the best fits to Eq. 3.

the properties of microphase separated structure of a sample at the final temperature. As shown in Fig. 4, each data set is well fitted to the Avrami equation with an exponent n=3 (see solid lines) except initial induction period. Detailed analysis using the nucleation and growth (NG) mechanism will be discussed in the next section.

In time-resolved SAXS measurements, the growth of I_{max} was monitored as a function of time after quenching the sample to each desired temperature. The results obtained are presented in Fig. 5a. The time evolution of I_{max} shows a similar trend as those of G' and G". As will be discussed in the next section, the growth of I_{max} shown in Fig. 5a is fitted to the Avrami equation with an exponent $n \approx 3$ for a shallow quench (T_{ODT}-T=11.8°C) and $n \approx 4$ for a deeper quench (T_{ODT}-T=20.4°C) respectively except the initial induction period. The best fits to the Avrami equation are shown as solid lines in Fig. 5a. As stated above, the initial induction period exists since the sample temperature in reality does not drop stepwise to a set temperature but rather change gradually over a short time period. This gradual temperature change of the sample with time can be clearly seen in Fig. 5b. The solid lines in Fig. 5b are the best fits to the following equation:

$$T(t) = T_m - (T_m - T_i)\exp(-t/\tau') \quad (3)$$

where T_i and T_m are the initial and final temperatures respectively, and τ' is the relaxation time of a given temperature drop. Data points are well fitted with this equation as shown in Fig. 5b. τ' values determined from the fitting were 41.0 sec for T_{ODT}-T=11.8°C and 31.2 sec for T_{ODT}-T=20.4°C, respectively. As expected, τ' value is smaller for a deeper quench. Comparison between Fig. 's 5a and 5b reveals out that the initial induction period in the time-evolution of I_{max} is essentially related to the thermal equilibration time of the sample.

3.3. Ordering Kinetics of 70/30 (w/w) SEBS/H1149 Mixture

In order to analyze the time-resolved rheological and scattering data obtained in present study in terms of the general nucleation and growth (NG) mechanism of the Avrami type, volume fraction of the ordered phase at a given time after a temperature quench, $\phi(t)$, should be known first. For the time-resolved rheology, the dynamic storage modulus at a given time can be expressed as a linear com-

bination of the initial and final storage modulus, G'_0 and G'_∞. Thus $\phi(t)$ can be defined as

$$\phi(t) = \frac{G'(t) - G'_0}{G'_\infty - G'_0} \tag{4}$$

For the time-resolved scattering, $\phi(t)$ is similarly defined as

$$\phi(t) = \frac{I_{max}(t) - I_0}{I_\infty - I_0} \tag{5}$$

The classical Avrami equation is then expressed as

$$\phi(t) = 1 - \exp[-(t/\tau)^n] \tag{6}$$

where τ is the relaxation time for the ordering and n is the Avrami exponent. The relaxation time is a quantitative measure of the ordering rate, which is usually expressed in terms of the half-time $t_{1/2}$:

$$t_{1/2} = (\ln 2)^{1/n}\,\tau \tag{7}$$

The Avrami exponent, n, yields qualitative information on growth dimensionality as well as nature of the NG mechanism. It is clear from Eq. 6 that the Avrami parameters can be obtained directly from the slope and the intercept of the Avrami plot of log(-log(1-ϕ)) versus log t.

The Avrami plots for the 70/30 (w/w) SEBS/H1149 mixture are constructed in Fig.'s 6 and 7 from each of the time-resolved rheological and SAXS data. While the Avrami plots from the time-resolved rheology show a slope of about 3 for all the given quench depths (see Fig. 6), those from the time-resolved SAXS demonstrate a slope of about 4 for a deeper quench as well as a slope of about

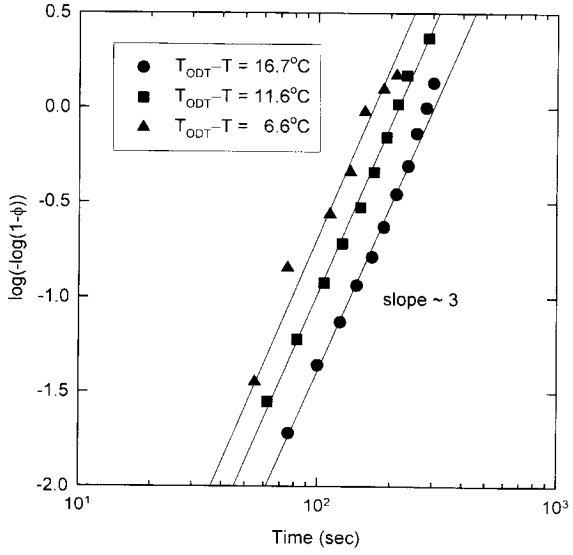

Fig. 6. Avrami plots obtained from the time-resolved rheology for different quench depths for 70/30 (w/w) SEBS/H1149 mixture.

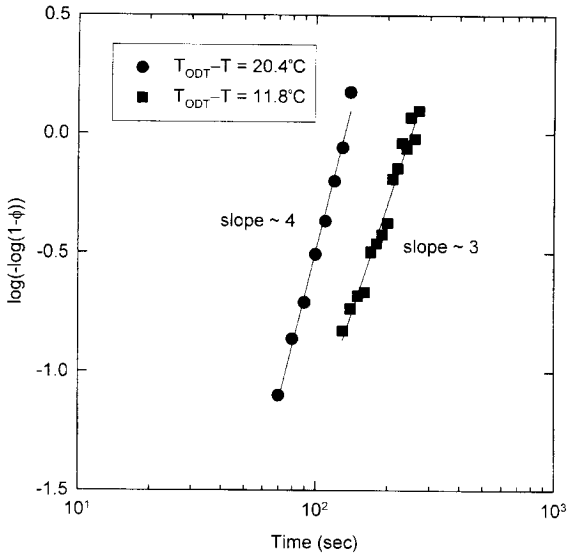

Fig. 7. Avrami plots obtained from the time-resolved SAXS for two quench depths for 70/30 (w/w) SEBS/H1149 mixture.

3 for a shallow quench (see Fig. 7). The curves in Fig.'s 6 and 7 shift to the left as the quench depth is increased since the ordering proceeds faster for a deeper quench. In order to compare the results from both time-resolved measurements, the Avrami parameters for the 70/30 (w/w) mixture obtained from both measurements are plotted as a function of quench depth, T_{ODT}-T, in Fig. 8: (a) the half-time versus quench depth and (b) the Avrami exponent versus quench depth. Note that the Avrami parameters measured from both rheology and SAXS agree well with each other for the same quench depth as can be seen in parts a and b of Fig. 8. The half-time for the 70/30 (w/w) mixture shown in Fig. 8a is shorter for a deeper quench as expected, indicating that the ordering proceeds faster for a deeper quench. The Avrami exponent shown in Fig. 8b was found to be about 3 for shallow quenches up to T_{ODT}-T=16°C and about 4 for further deeper quench.

The Avrami exponent of n=3 for a shallow quench indicates that the ordering of the 70/30 (w/w) mixture proceeds by the *heterogeneous nucleation and growth* of three-dimensional grains of the microdomain structure. The change of the slope from 3 to 4 in going from a shallow to a deeper quench may be the sign of a transition in the ordering kinetics of the mixture; from the heterogeneous NG mechanism to the spinodal decomposition (SD) mechanism. Experimental observations similar to the present study were recently reported by Floudas *et al.*[18]. They investigated the ordering kinetics of SI diblock, SI_2 simple graft copolymer and SIB terpolymer using rheology as well as SAXS. They observed that for a shallow

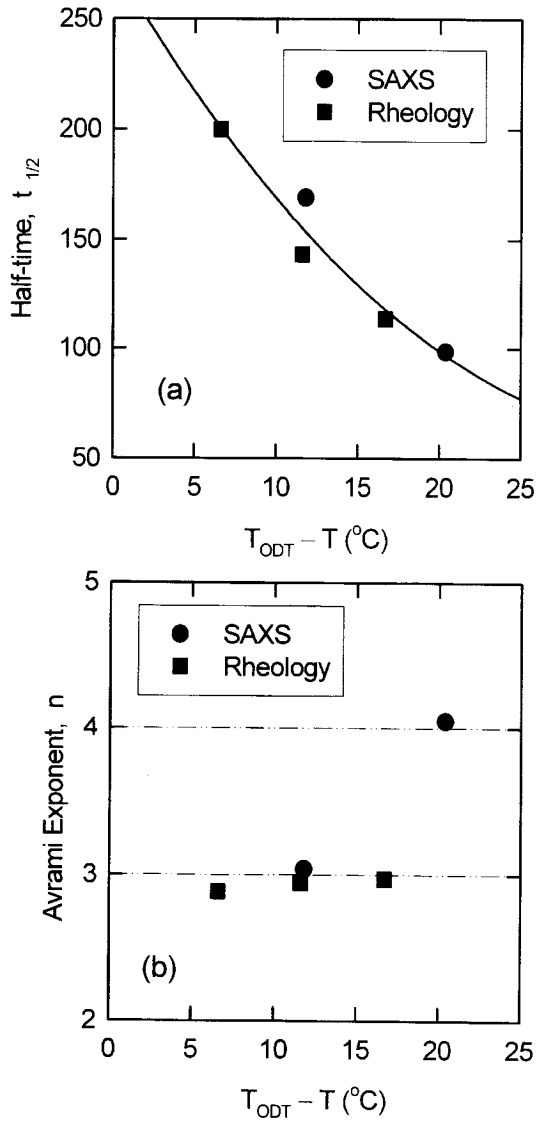

Fig. 8. Avrami parameters obtained from both time-resolved SAXS and time-resolved rheology for 70/30 (w/w) SEBS/H1149 mixture as a function of quench depth, T_{ODT}-T: (a) half-time versus quench depth and (b) Avrami exponent versus quench depth.

quench the Avrami exponent n was 3 and ln $t_{1/2}$ was linearized better when plotted against δ^{-1} than δ^{-2} (δ is the degree of undercooling defined in Eq. 1). Based on these facts, they concluded that all the copolymers used in their study proceed by the heterogeneous NG mechanism for a shallow quench. This is quite reasonable since n equals 4 and $t_{1/2}$ is proportional to δ^{-2} in the case of homogeneous nucleation, whereas $t_{1/2}$ is proportional to δ^{-1} in the case of heterogeneous nucleation[14]. They also noted that the change of the Avrami exponent of their copolymers from 3 to 4 in going from a shallow to a deeper quench could imply the ordering process due to SD for a deeper quench. Unfortunately, we now have only few data sets to plot $t_{1/2}$ against δ^{-2} (in the case of homogeneous nucleation) or δ^{-1} (in the case of heterogeneous nucleation). More detailed study on this aspect will be the subject of our further study. Since SEBS triblock copolymer used in present study is highly asymmetric (f_{PS}=0.242), however, it is quite unlikely for the mixture to order by the homogeneous NG mechanism. It is known that there exists a huge nucleation barrier for highly asymmetric block copolymers as can be seen in Eq. 2. In addition to this, the homopolymer present in the mixture may act as a nucleating agent during the ordering process in the case of a shallow quench.

4. Conclusion

We employed both *time-resolved* rheological and *synchrotron* small-angle X-ray scattering (SAXS) measurements to investigate the ordering kinetics as well as the order-disorder transition (ODT) of a 70/30 (w/w) mixture of polystyrene-*block*-poly(ethylene-*co*-butylene)-*block*-polystyrene (SEBS), Kraton G1652, and a commercial tackifier, Hercotac 1149 (H1149). T_{ODT} of the mixture was first determined independently by each static measurement. Time-resolved measurements were then carried out by quenching the sample from disordered to ordered state, thus enabling us to monitor the ordering process as a function of time. In order to analyze the time resolved data of our triblock copolymer/homopolymer mixture system, we applied the nucleation and growth (NG) mechanism of the Avrami class which has been used by many investigators to analyze the ordering kinetics of pure block copolymers. Time evolutions of G' and G" as well as I_{max} for the 70/30 (w/w) mixture after a given quench were well described by the NG mechanism except the initial induction period. The Avrami exponents and ordering half-times obtained from both time-resolved measurements were in good agreement with each other for the same quench depth. Ordering half-time was found to gradually decrease as the quench depth was increased, indicating that the ordering proceeds faster for a deeper quench. The Avrami exponent was found to have a sudden change from about 3 to 4 in going from a shallow to a deeper quench. This implies that the ordering of the 70/30 (w/w) mixture may proceed *via* the heterogeneous NG mechanism for a shallow quench, whereas there exists a transition in the ordering kinetics into the spinodal decomposition (SD) mechanism when the sample is further quenched.

Acknowledgments

Experiments performed at Pohang Light Source (PLS) were supported by MOST and POSCO. We are also very grateful to Y. J. Park for his assistance during the SAXS experiments at PLS.

References

1. M.D. Whitmore and J. Noolandi, *Macromolecules,* **18**, 2486 (1985).
2. H. Tanaka, H. Hasegawa, and T. Hashimoto, *Macromolecules,* **24**, 240 (1991).
3. A.M. Mayes, T.P. Russell, S.K. Satija, and C.F. Majkrzak, *Macromolecules,* **25**, 6523 (1992).
4. L. Leibler, *Macromolecules,* **13**, 1602 (1980).
5. G.H. Fredrickson and E. Helfand, *J. Chem. Phys.,* **87**, 697 (1987).
6. J.H. Rosedale and F.S. Bates, *Macromolecules,* **23**, 2329 (1990).
7. F.S. Bates, J.H. Rosedale, and G.H. Fredrickson, *J. Chem. Phys.,* **92**, 6255 (1990).
8. N. Sakamoto and T. Hashimoto, *Macromolecules,* **28**, 6825 (1995).
9. C.D. Han, J. Kim, and J.K. Kim, *Macromolecules,* **22**, 383 (1989).
10. C.D. Han, D.M. Baek, J.K. Kim, T. Ogawa, N. Sakamoto, and T. Hashimoto, *Macromolecules,* **28**, 5043 (1995).
11. T. Hashimoto, K. Kowsaka, M. Shibayama, and S. Suehiro, *Macromolecules,* **19**, 750 (1986).
12. T. Hashimoto, K. Kowsaka, M. Shibayama, and H. Kawai, *Macromolecules,* **19**, 754 (1986).
13. T. Hashimoto, *Macromolecules,* **20**, 465 (1987).
14. G.H. Fredrickson and K. Binder, *J. Chem. Phys.,* **91**, 7265 (1989).
15. K. Binder, *Physica A,* **213**, 118 (1995).
16. T. Hashimoto and N. Sakamoto, *Macromolecules,* **28**, 4779 (1995).
17. G. Floudas, T. Pakula, E.W. Fischer, N. Hadjichristidis, and S. Pispas, *Acta Polymer.,* **45**, 176 (1994).
18. G. Floudas, N. Hadjichristidis, H. Iatrou, T. Pakula, and E.W. Fischer, *Macromolecules,* **27**, 7735 (1994).
19. G. Floudas, S. Pispas, N. Hadjichristidis, T. Pakula, and I. Erukhimvich, *Macromolecules,* **29**, 4142 (1996).
20. G. Floudas, D. Vlassopoulos, M. Pitsikalis, N. Hadjichristidis, and M. Stamm, *J. Chem. Phys.,* **104**, 2083 (1996).
21. J.L. Adams, D.J. Quiram, W.W. Graessley, R.A. Register, and G. R. Marchand, *Macromolecules,* **29**, 2929 (1996).
22. M. Schuler and B. Stühn, *Macromolecules,* **26**, 112 (1993).
23. B. Stühn, A. Vilesov, and H.G. Zachmann, *Macromolecules,* **27**, 3560 (1994).
24. C.R. Harkless, M.A. Singh, S.E. Nagler, G.B. Stephenson, and J. L. Jordan-Sweet, *Phys. Rev. Lett.,* **64**, 2285 (1990).
25. E. Domany and S.E. Nagler, *Physica A,* **177**, 301 (1991).
26. T. Ogawa, N. Sakamoto, T. Hashimoto, C.D. Han, and D.M. Baek, *Macromolecules,* **29**, 2113 (1996).